



# Prediction of river bank erosion and protection works in a reach of Chenab River, Pakistan

Muhammad Ashraf<sup>1</sup> · Abdul Sattar Shakir<sup>2</sup>

Received: 31 January 2017 / Accepted: 15 March 2018 / Published online: 2 April 2018  
© Saudi Society for Geosciences 2018

## Abstract

The impacts of floods on river bank erosion are generally significant in the alluvial river reaches. This paper presents the prediction of the river bank erosion along the right bank in the reach of Chenab River (starting from downstream of Marala Barrage) where excessive erosion had been reported. The bank erosion is predicted due to flow/flood events of 2010 by coupling the output from the two-dimensional numerical model to the excess shear stress approach. The predicted bank erosion was compared with the one estimated from Landsat images. The Landsat ETM+ images were processed in the ArcGIS software to assess the external bank erosion. The results show that the excess shear stress approach underpredicts the bank erosion. Therefore, the erodibility coefficient was modified by forcing the best agreement between predicted and estimated (i.e., from Landsat images) bank erosion which was used for further analysis. The results reveal that coupling the output from the numerical model to the excess shear stress approach (by modifying the erodibility coefficient) predicts the river bank erosion with a reasonable level of accuracy, thus helpful to identify the locations for the protection works. The predicted river bank erosion presents good coefficient of determination ( $R^2$ ) of 0.82 when compared with the estimated bank erosion from Landsat images. The findings of the present study will help to implement the river protection works at the identified locations in the selected reach of River Chenab and will also act as a guideline for similar river reaches.

**Keywords** River bank erosion · Landsat images · Excess shear stress · Erodibility coefficient

## Introduction

The river bank erosion causes significant environmental and economic problems such as loss of agricultural land and infrastructure along the river banks. The excessive river bank can also contribute into the total sediment load in rivers (Ercan and Younis 2009). The Chenab River widened by about 6% due to bank erosion downstream of Marala Barrage which caused the land loss of about 4.2 million m<sup>3</sup> along the river bank (Ashraf et al. 2016). Similarly, river bank erosion

supplies a significant proportion of the total sediment load for many other rivers (see for example, Sekely et al. 2002; Thoma et al. 2005).

The river configuration, hydrology, and soil stratification of the banks complicates the assessment of bank erosion and identification of the locations more susceptible to erosion along the river bank. For cohesive river banks, the erosion is principally a function of discharge which increases the rate of change in river width as the distance increases downstream. But at a particular section, the formation of sand bars and central island cause the increase in the external banks erosion which increases the rate of change of width (Knighton 1974; Akhtar et al. 2011). River bank erosion strongly depends on the event peak discharge (Hooke 1979). The combined actions of different physical processes, e.g., weathering, fluvial erosion, and geotechnical instability, cause bank erosion (Thorne 1982; Lawler 1992). In addition, some other factors such as the soil properties, the frequency of freeze–thaw, the stratigraphy of the bank structure, the type and density of vegetation, and the grain size of the bed sediment at the toe of the bank significantly influence the erosion processes.

✉ Muhammad Ashraf  
ashraf\_uaf@hotmail.com

Abdul Sattar Shakir  
shakir@uet.edu.pk

<sup>1</sup> Centre of Excellence in Water Resources Engineering (CEWRE), University of Engineering & Technology, Lahore, Pakistan

<sup>2</sup> Civil Engineering Department, University of Engineering & Technology, Lahore, Pakistan

Julian and Torres (2006) reported that the four flow properties controls the hydraulic erosion rates of cohesive riverbanks: (1) magnitude, (2) duration, (3) event peak, and, (4) variability. The banks with low cohesion strongly depend on the intensity of all peak events rather than just the highest peak, moderately cohesive banks on event peak and minimally cohesive banks on variability (number of discharge peaks). Darby et al. (2007) also found the maximum fluvial erosion on event peak. Luppi et al. (2009) concluded that the fluvial erosion is dominant during the flood events with single peak and the mass failure occurred during the multi-peaked prolonged events.

The excess shear stress approach (Eq. 1) is most commonly used to predict hydraulic erosion rates of cohesive river banks (e.g., Osman and Thorne 1988; Darby and Thorne 1996; Darby et al. 2007; Luppi et al. 2009; Hanson and Simon 2001; Ercan and Younis 2009; Simon et al. 2009). The relationship developed by Partheniades (1965) assumes that the amount of hydraulic erosion is a function of the magnitude of excess shear stress ( $\tau_a - \tau_c$ ) (Eq. 1):

$$E = k(\tau_a - \tau_c)^a \quad (1)$$

where “E” is lateral erosion rate in meters per second, “k” is an erodibility coefficient in cubic meter/Newton second, “ $\tau_a$ ” is applied shear stress by flow in Pascal, and “ $\tau_c$ ” is critical stress in Pascal.

The excess shear stress approach is simple and requires the calculations of erodibility parameters and boundary shear stress from the field observations for the accurate estimation of river bank erosion. These parameters are all highly variable. Theoretical determination of critical shear stress for cohesive materials is very complex because it depends on several factors including clay and organic content, and the composition of interstitial fluids (Arulanandan et al. 1980; Grissinger 1982). Consequently, better fluvial erosion predictions depend on how accurately these parametric values are estimated.

Many researches have reported the inverse relationship between erodibility coefficient and critical shear stress (Thoman and Niezgod 2008). Initially, the relationship between erodibility coefficient and critical shear stress was found by Hanson and Simon (2001) for stream beds. Subsequently, the relationship was updated for stream banks by Simon et al. (2011). Daly et al. (2013) proposed a new approach to analyze the data collected during the jet erosion test and developed a new relationship between erodibility coefficient and shear stress.

Simon et al. (2009) used the same relationship for erodibility coefficient which was developed by Hanson and Simon (2001). The results showed that the 13.6% bank erosion occurred by fluvial erosion which is calculated by using the excess shear stress approach whereas the remaining erosion

resulted due to the mass failure. Similarly, Rinaldi et al. (2008) concluded that the 30% of the erosion occurred due to fluvial erosion and the major bank erosion occurs due to pore water and hydrostatic confining pressure between the drawdown and rising phases of the multi-peaked flow events. Interestingly, they found the outer bank shear stress out of phase with the river stage. They suggested these conditions due to the specific geometric configuration of the channel bend. Ercan and Younis (2009) successfully predicted the bank erosion using the excess shear stress approach without any changes in the Hanson and Simon (2001) approach for erodibility coefficient determination. Moreover, the bank erosion models such as Bank Stability and Toe Erosion Model (BSTEM) and CONCEPT also uses the Hanson and Simon (2001) relationship to estimate bank erosion. However, many researchers have developed the different relationship between these two parameters (e.g., Clark and Wyn 2007; Darby et al. 2007; Thoman and Niezgod 2008).

Review of above-cited studies indicates that the approach, relatively simple and robust, can be used to address these problems for implementation of river protection works by considering the relationship of erodibility coefficient and critical shear stress and excess shear stress for individual peak events (i.e., intensity and duration). Also, the main focus of the researchers has been remained on the accurate estimation of river bank erosion. Only, few researchers have used the excess shear stress approach to analyze the impact of structural measures on river bank erosion. Therefore, for this study, the specific objectives are to: (1) develop the relationship between erodibility coefficient and critical shear stress for the selected river reach, (2) predict the bank erosion using the excess shear stress approach, and (3) identify the locations more susceptible to erosion.

## Materials and methods

### Study area

The reach of the River Chenab, starting from downstream of Marala Barrage near Sialkot (Pakistan), is selected for the prediction of the bank erosion. The river reach can be categorized as braided which includes semi-stable vegetated island, sand bars, and channels (Fig. 1).

The catchment area above Marala Barrage has moderate to high vegetation cover and the major landuse is grassland because it receives rainfalls almost in each month of the year which keeps the vegetation growing along the hill slopes (Rehman et al. 2012). The summary of the characteristics of the study reach and hydrology of the river at upstream of Marala Barrage is given in Table 1.

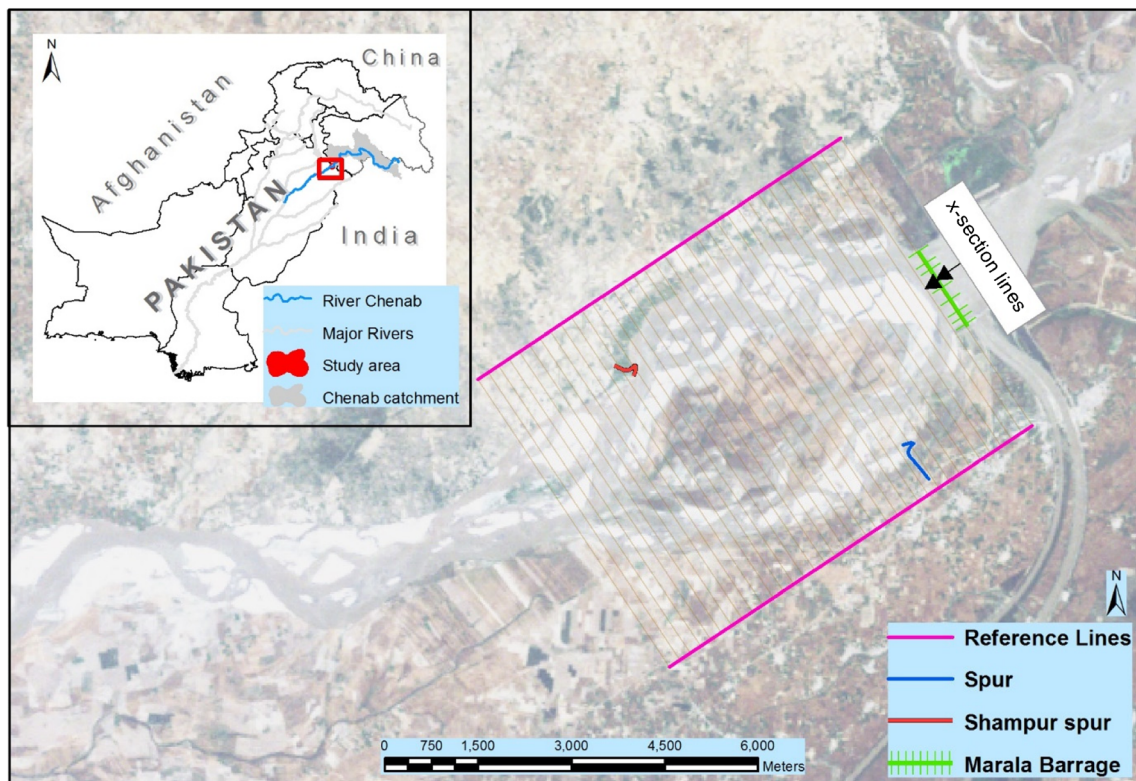


**Fig. 1** Study area map with locations of Marala Barrage, groynes, and reference line from where the bank erosion was estimated using Landsat images

The soil in the Marala-Alexandra reach is transitory from sediment plains of the Pir Punjal range to flatter flood plains of Punjab (Awan 2003). The river banks are highly susceptible to erosion due to the higher proportion of the silt and clay particles in the bank material. The river banks in the middle part of the selected river reach have witnessed the erosion over multiple times. The river bank erosion occurs, especially along the right bank, during the monsoon season (July to September) due to the flood events. The average bank erosion rate of the selected reach is  $34.3 \text{ m}^{-1}$  which lies in the upper limit of the global bank erosion rate. The left bank is stable and experiences negligible erosion since the construction of a big groyne during 2005–06 (Ashraf et al. 2016).

### Discharge and water level during 2010

Flow in the River Chenab significantly depends on the snow-melt contribution during summer. Maximum snowmelt experiences in the month of July whereas high magnitude floods generate due to monsoon rainfalls in the catchment. There is almost no control over the Chenab River in Pakistan (Tariq and Giesen 2012). Regular discharge and gauge height measurements are conducted at downstream and upstream of Marala Barrage. The Chenab River experienced medium to high flood events during the monsoon season of 2010 as reported by the Punjab Irrigation Department (PID). The maximum flood peak was observed on August 6, 2010 (Fig. 2).

**Table 1** Catchment area at Marala Barrage. Key features of the study area and hydrology of the river at Marala Barrage

Description	Value	Unit
Catchment area	32,670	km <sup>2</sup>
Mean water yield	25.17	km <sup>3</sup> y <sup>-1</sup> (Tariq and Giesen 2012)
Mean annual discharge	918.0	m <sup>3</sup> s <sup>-1</sup>
Average river width	3.5	km
Reach length	7	Km
Average bank height	5	m
Mean elevation of the study area	240.0	m.a.s.l
Mean river bed slope	0.2	%

**Fig. 2** Flood events at Marala Barrage during the monsoon of 2010

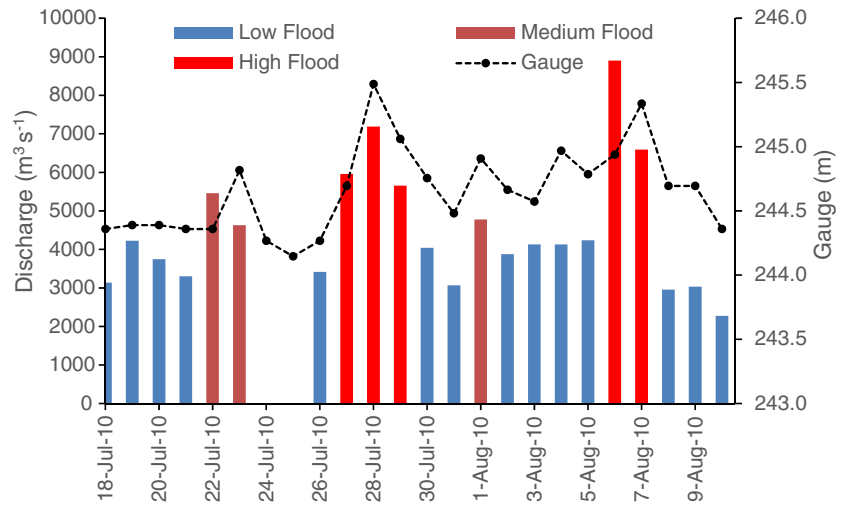


Figure 2 shows the instantaneous flood peaks and average gauge height downstream of Marala Barrage during the monsoon season.

**Satellite data and images analysis**

Analysis of images in the GIS software is an important technique to estimate the river bank erosion and have been widely used by many researchers (e.g., Khan and Islam 2003; Takagi et al. 2007; Baki and Gan 2012; Mount et al. 2013, and Wang et al. 2014). For this study, Landsat images of Enhanced Thematic Mapper plus (ETM+) with a 30-m resolution were analyzed to calculate the bank erosion. The selected images were acquired approximately before and after the flows/floods simulation period in order to calculate the river bank erosion. For this study, images of 2010 acquired on June 27 and October 9 were used for the analysis.

Images of visible and near infra-red (NIR) ranges of electromagnetic spectrum were used for analysis. Because, these bands enables the vegetation boundary along the river to identify the outer bank line as discussed by Wang et al. (2014). In addition, Iso Cluster Unsupervised classification (ICUS) was also used to identify the different features like main river channel, island/bela, and sandbars. Details of images used and methodology adopted to estimate the river bank erosion can be found in Ashraf et al. (2016).

**Numerical method**

The CCHE (Centre for Computational Hydrosiences and Engineering) two-dimensional model was used to estimate the shear stress for this study. The numerical model results were coupled with the excess shear stress approach to estimate the bank erosion. The numerical model (CCHE2D) is a two-dimensional hydrodynamic and sediment transport model designed to simulate unsteady flows in open channel. The model

is based on the finite element grid system. The depth-integrated two-dimensional equations govern the water flow computation. The governing equations (Eqs. 2 and 3) for open channel flow can be written in the following form in a Cartesian coordinate system:

$$\frac{\partial u}{\partial t} + u \frac{\partial u}{\partial x} + v \frac{\partial u}{\partial y} = -g \frac{\partial \eta}{\partial x} + \left[ \frac{1}{h} \frac{\partial}{\partial x} (h\tau_{xx}) + \frac{\partial}{\partial y} (h\tau_{xy}) \right] - \frac{\tau_{bx}}{\rho h} + f_{cor} v \tag{2}$$

$$\frac{\partial v}{\partial t} + u \frac{\partial v}{\partial x} + v \frac{\partial v}{\partial y} = -g \frac{\partial Z}{\partial y} + \left[ \frac{1}{h} \frac{\partial}{\partial x} (h\tau_{yx}) + \frac{\partial}{\partial x} (h\tau_{yy}) \right] - \frac{\tau_{by}}{\rho h} - f_{cor} v \tag{3}$$

where  $u$  and  $v$  are the depth-integrated velocity components in the  $x$  and  $y$  directions, respectively;  $g$  is the gravitational acceleration;  $z$  is the water surface elevation;  $\rho$  is water density;  $h$  is the local water depth;  $f_{cor}$  is the Coriolis parameter;  $\tau_{xx}$ ,  $\tau_{xy}$ ,  $\tau_{yx}$ , and  $\tau_{yy}$  are the depth-integrated Reynolds stresses; and  $\tau_{bx}$  and  $\tau_{by}$  are shear stresses on the bed and flow surfaces.

Free surface elevation for flow is calculated by the continuity equation (Eq. 4):

$$\frac{\partial Z}{\partial t} + \frac{\partial(hu)}{\partial x} + \frac{\partial(hv)}{\partial y} = 0 \tag{4}$$

The turbulence Reynold’s stresses are approximated according to Bousinesq’s assumption. Shear stresses on bed can be evaluated by two approaches in the model: (1) depth-integrated logarithmic law and (2) by utilizing Manning’s coefficient. In the first approach, shear stresses are obtained by using Eqs. 5 and 6:

$$\tau_{bx} = \frac{1}{8} \rho f_c u U \tag{5}$$

$$\tau_{by} = \frac{1}{8} \rho f_c v U \quad (6)$$

where  $f_c$  is the Darcy Weisbach coefficient which can be obtained after the calculation of shear velocity ( $u_*$ ) (Van Rijn 1993) and  $U = \sqrt{u^2 + v^2}$ . The second approach utilizes the Manning's coefficient to calculate shear stresses (Eqs. 7 and 8):

$$\tau_{bx} = \frac{1}{h^{0.667}} \rho g n^2 u U \quad (7)$$

$$\tau_{by} = \frac{1}{h^{0.667}} \rho g n^2 v U \quad (8)$$

The second approach for the calculation of shear stresses is recommended for practical applications because it is the most efficient and lump the effects of bed forms, channel geometry, sediment size and vegetation, etc. The details can be found in Jia and Wang (2001). The methodology used to estimate the excess shear stress and bank erosion rate calculation are described in the subsequent section.

### Numerical modeling and model settings

The simulation of flows using the two-dimensional numerical model completes in two steps: (1) the generation of mesh and (2) simulation of model by defining the initial and boundary conditions and parameters setting. The CCHE2D finite element model solves depth-integrated momentum equations for flow simulation with different turbulence closure models. The details of the flow equations, turbulence closure, and shear stress approximation are given in the previous section ("Numerical method" section). Bank erosion was computed using the excess shear stress approach by coupling the numerical model results which estimated the shear stress.

The morphology data set for the modeling was taken from the river survey conducted during 2009–10. The survey was conducted along the cross sections of the river at 457 m (1500 ft) interval. The cross-section data covers the width of river sections from the left external river bank to the right river bank, covering the entire river width. Topographic data contained the measured bed elevation or bathymetric (bed elevation) data with no coordinates. Therefore, the available topographic data was geo-referenced in the ArcGIS software prior to loading in the numerical model. Cross section lines were digitized (using ArcGIS) at a specified distance from Marala Barrage as these were measured during survey. The surveyed points were automatically generated on the digitized cross section lines by using the route tool available in the linear referencing tool box of the software. Latitude and longitude fields were added in the attribute table of the shape file of automatically generated points, and these coordinate values were using the field calculator tool of ArcGIS. The extracted

latitude, longitude, and elevation values of the points were then used to prepare the file in a required format (i.e., .mesh\_xyz) for the CCHE mesh generator.

Study region was defined in CCHE Mesh generator by digitizing the first and second boundary of the river reach along the external banks of the river using the loaded topographic data. Color variation of points (loaded topographic data) along with the shape files of temporary island helped in digitizing the boundaries in the mesh generator model (Fig. 3).

Algebraic mesh was generated by specifying the 88 lines in the J direction (cross sections) and 44 lines in the I direction (longitudinal sections) after digitizing the flow domain and the island in the river reach. Different numerical mesh generation options are available for smoothing of generated mesh. For this study, TTM orthogonal mesh was selected for smoothing of generated mesh and then different parameters were evaluated to assess the quality of mesh. Generated two-dimensional mesh was then converted into three-dimensional mesh using topographic data which was imported in the CCHE-Mesh generator in form of point elevations.

### Initial and boundary conditions

In this study, two separate simulations were done due to the limited computational power of processing. The daily flow data measured at Marala Barrage was used as input hydrograph in two separate simulations, i.e., February 8 to July 19, 2010 and July 18 to August 10, 2010, respectively. For the second period of simulation, discharge data (i.e., actual magnitude and duration) of each flood event was also considered in addition to the daily flow data.

The initial water level is of key importance as the model run do not execute if the initial water level is too low as it will leave too many dry nodes. For this study, the initial water level was taken as 245.3 m.a.s.l. The water level and the open boundary condition were taken as outlet boundary condition to allow the model to calculate the water level based on kinematic wave condition.

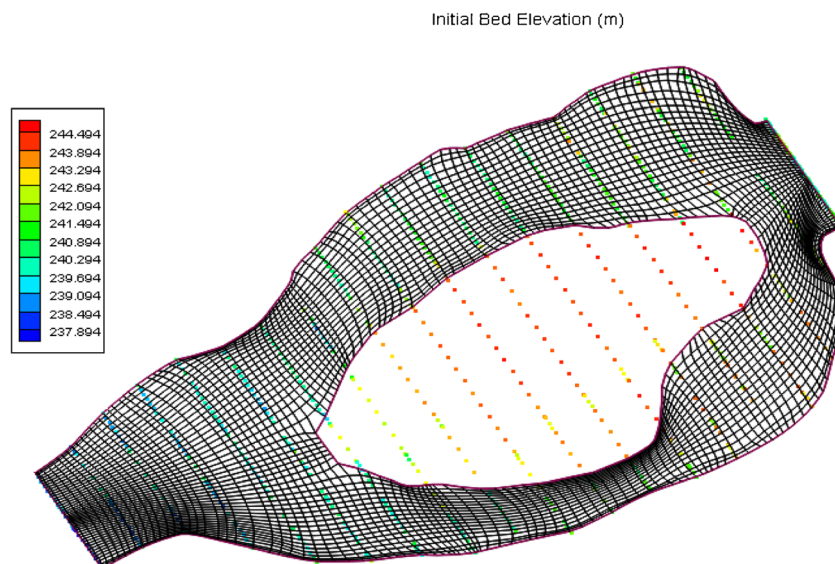
Bed roughness for island, for semi-stable sand bar, and the river channel were estimated using the Strickler's formula (Eq. 9):

$$n = 0.04 d_{50}^{0.167} \quad (9)$$

where  $n$  = Manning's roughness coefficient,  $d_{50}$  = mean diameter of the bed material taken from the gradation curves for river bed and sand bars/islands.

Manning's roughness coefficient values for river and islands were found to be 0.033 and 0.032, respectively. The negligible difference in roughness coefficient was found due to the narrow range of sediment sizes as most of the sediment was categorized as medium sand based on USDA soil classification.

**Fig. 3** Digitized domain boundaries and the island in CCHE Mesh generator on topographic data



### Bank erosion rate estimations using the excess shear stress approach

The bank erosion is predicted by coupling the numerical model results with the excess shear stress approach. Shear stresses were calculated by numerical model simulation of the mean daily flows/flood events basis. The critical shear stress for river bed material size particles is calculated from Shields' curve (Shields 1936) which was  $0.018 \text{ N m}^{-2}$  and the value of the exponent "a" is taken to be 1.

A sediment particle on a sloping river bank is less stable than one on the bed (Ikeda 1982). The relationship (i.e., Eq. 10) developed by Lane (1955) was used to account for the gravity force which tend to move the particles downward on sloping river bank:

$$\frac{\tau_{wc}}{\tau_c} = \cos\theta_1 \sqrt{\left(1 - \frac{\tan\theta_1}{\tan\phi}\right)^2} \quad (10)$$

where  $\theta_1$  is the bank slope and  $\tan \phi$  is the angle of repose for the sediment which was estimated as  $32^\circ$  based on size of the sediment. The angle of repose of a particle can be found in Lane (1955) based on the particle size of the river bank. The erodibility coefficient ( $K$ ) was estimated using the relationship developed by Hanson and Simon (2001) as given in Eq. 11:

$$K = 2 \cdot 10^{-7} \tau_c^{-0.5} \quad (11)$$

The erodibility coefficient ( $K$ ) is found by substituting the value of the critical shear stress in Pa. When all the parameters (i.e., erodibility coefficient, critical shear stress) for the particles of bank material were estimated through Eqs. 10–11 and the applied stress through numerical model simulation were calculated, then Eq. 1 was used to estimate the bank erosion.

The relationship for the erodibility coefficient (given in Eq. 11) was revised for the study reach via bank erosion calibration (i.e., by forcing best agreement between measured and calculated river bank erosion).

## Results and discussion

### Flow velocities and shear stress computations

Because the prediction of river bank erosion is based on the excess shear stress, therefore, the model was run to estimate the bed shear stresses along the bank for each flood peak event for the selected duration (February 28 to August 10, 2010). Contours of the velocity magnitude along with velocity vectors for two flood peaks predicted with the model are shown in Fig. 4. Results show that the maximum velocity occurs near the nose of the Shampur groyne and reaches up to 2.8 m/s (Fig. 5). The groyne at Shampur actually reduces the flow cross sectional area, thus causes the maximum velocities at this region. The flow velocities remain higher in the right branch channel than the left, thus allows the maximum discharge to pass from this side. Therefore, the river cross sections of the right side channel are also deeper than the left. The contours also shows that the flow velocities are low upstream of the groyne located along the left bank. But downstream of the groyne, the flow velocities are higher due to the reduction in the flow area.

The bed shear stresses for the study reach calculated through numerical model simulation for each of the flood peak/flows are shown in Fig. 6. The maximum shear stresses are also found at the nose of Shampur Groyne followed by the stresses downstream of the groyne along the left river bank.

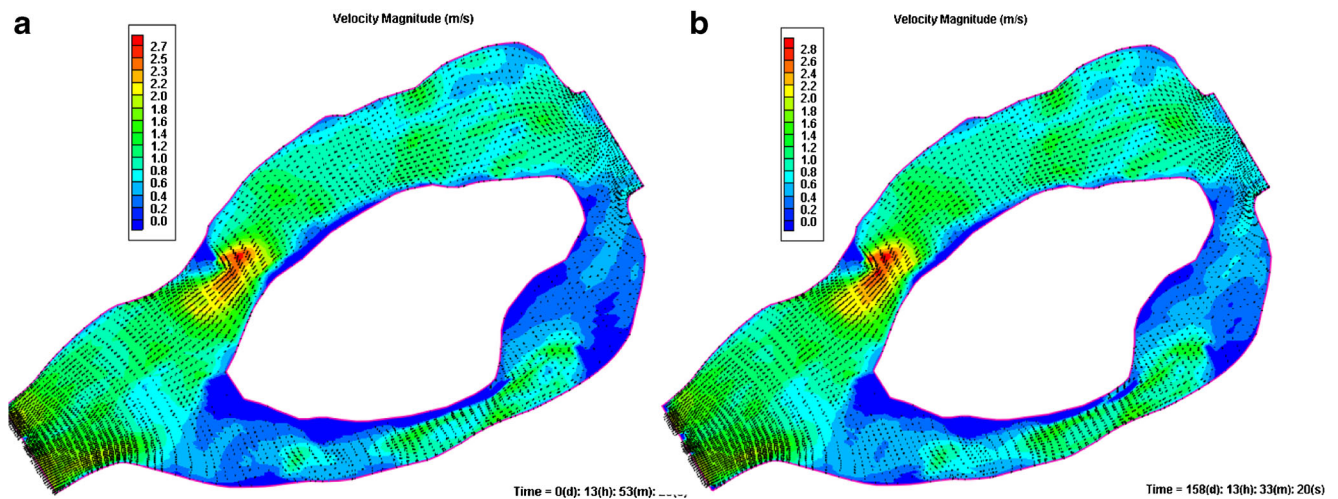


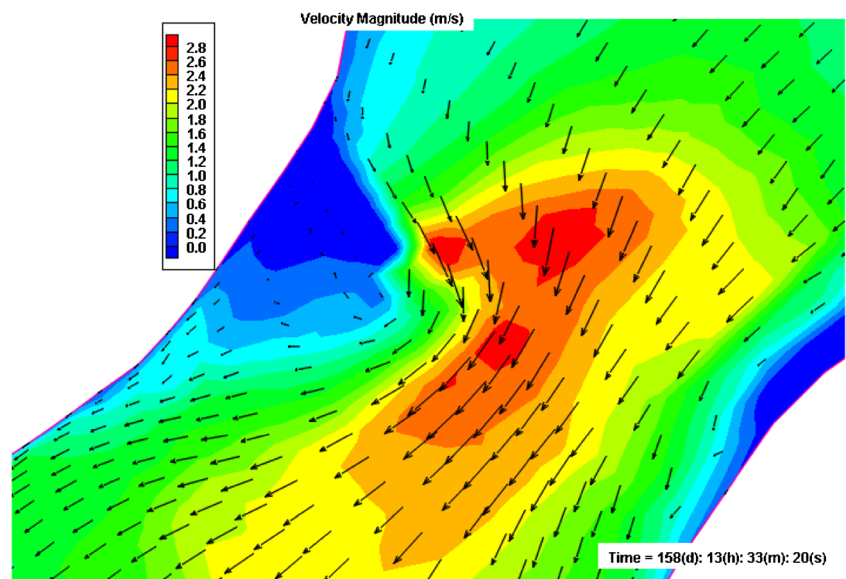
**Fig. 4** a Velocity magnitude contours and vectors during discharge of 4152 m<sup>3</sup>/s at 14 h of inflow. b Velocity magnitude contours and vectors during discharge of 4223 m<sup>3</sup>/s at end of simulation time

The groynes on both sides of the river banks led to increase the shear stresses similarly as they induced increased flow velocities. Moreover, similar pattern of shear stresses were found for the whole study reach due to each flood event as was found for the flow velocities. The critical shear stress was calculated using the shield’s curve (1936) by using the median sediment size. The critical shear stress for the medium sand particles was estimated as 0.018 N/m. The critical shear stress for particles on banks is not same as for the one on the bed of the river. Therefore, Eq. 10 was used to estimate the critical shear stress for particles on the river bank. The critical shear stress for the median size particles on the bank is estimated as 0.011 N/m.

The shear stress along the right river bank is plotted in Fig. 7. The maximum shear stress is computed at a distance of about 2500 m downstream of Marala barrage as 4.0 N/m<sup>2</sup>.

From Fig. 7, three locations can be identified for maximum shear stresses at a distance of 2500, 3450, and 4720 m, respectively. The stream velocities are significantly increased in the middle and the downstream section of the selected river reach due to constriction of channel width. The width of channel along the right bank was reduced due to the Shampur groyne. The reduction in flow cross section area causes the flow to accelerate in the main river channel. Normally, the high turbulence conditions occur near the nose of the groyne. The similar findings were observed by Ercan and Younis (2009). At these locations, the possibility of the bank erosion reduced due to the placement of groynes. The groynes also cause the recirculation zone. The groynes reduce the magnitude of shear stresses near the banks and increase of shear stress in the main river channel. No erosion at the downstream section of the groynes may be suggested due to sedimentation because the

**Fig. 5** Velocity magnitude contours and vectors near the Shampur Groyne for the discharge of 4223 m<sup>3</sup>/s during end of simulation time



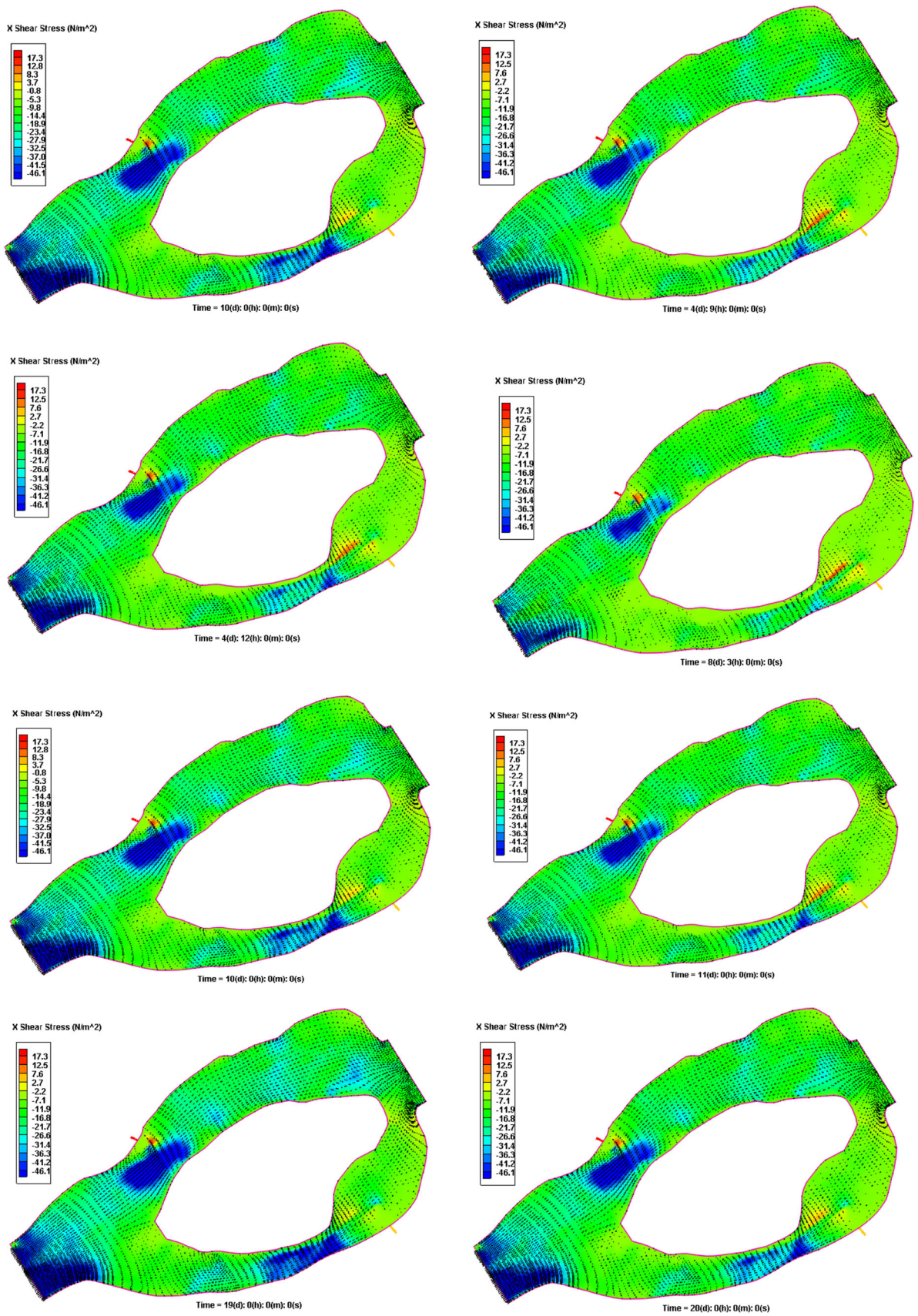
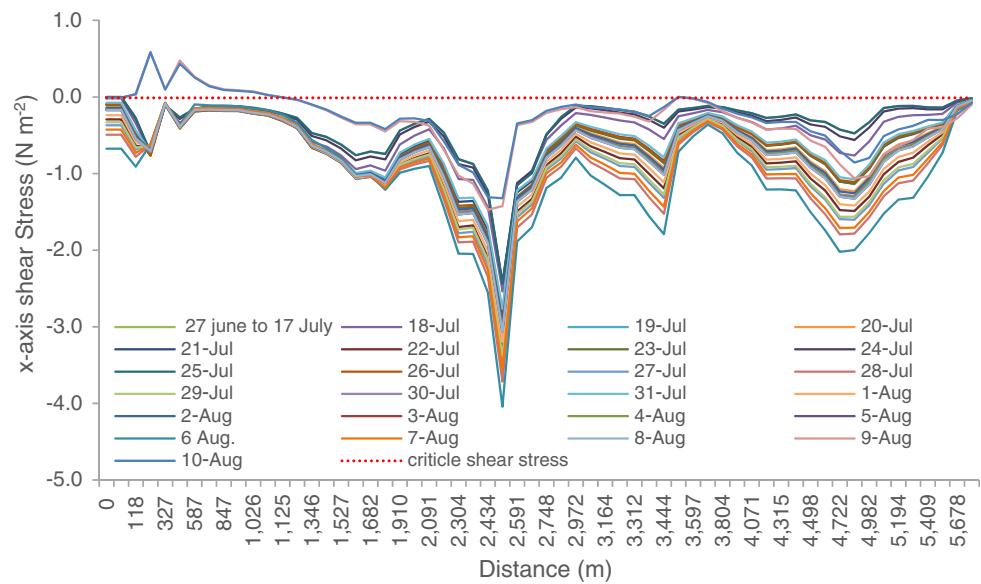


Fig. 6 Shear stress along x direction with velocity contours

**Fig. 7** The x-axis shear stresses along the right bank



presence of the recirculation zone favors the sedimentation, eventually to rehabilitation of the eroded bank (Ercan and Younis 2009). These findings were also confirmed during the field visit (Fig. 8).

**Prediction of Bank erosion**

Figure 9 shows the estimated bank erosion rate along the right bank for the river Chenab downstream of Marala Barrage. The erosion rate is based on the equations established by Partheniades (1965) and Hanson and Simon (2001). The maximum erosion along the right bank is predicted to be 18.7 m at a distance of about 2500 m downstream of the Marala Barrage. The values predicted by the excess shear stress approach were about 4.5 times lesser than calculated from remote sensing images. Similar findings of underestimation for bank erosion were reported by Clark and Wynn (2007), where

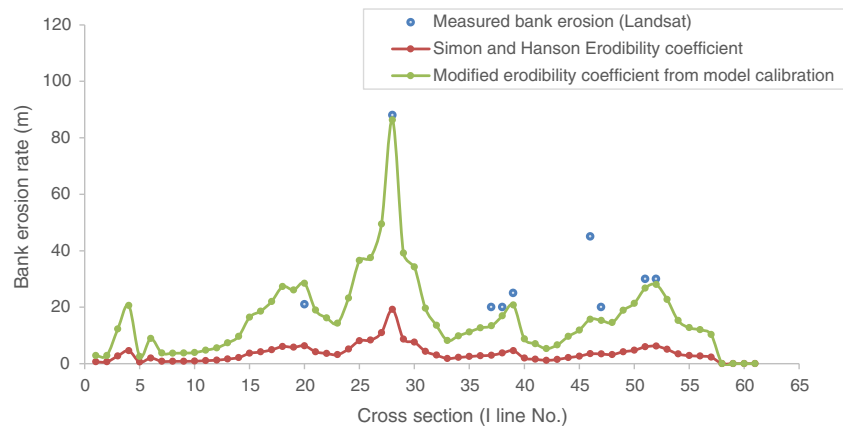
the measured erosion rates were two times more than estimated by Hanson and Simon relation (Eq. 12). Luppi et al. (2009) and Simon et al. (2009) also found the different percentage of bank erosion estimated by excess shear stress approach and attributed the other bank erosion mechanism in their findings.

Determination of soil erodibility coefficient is not an easy task due to complexity of inter-particle forces (Simon and Collison 2001). The soil properties such as dispersion ratio, soil pH, percent organic matter, etc., are responsible for different erodibility and critical shear stress. Therefore, multiple linear regression relationship was developed by Thoman and Niezgodna (2008) for the better estimation of the critical shear stress to modify the critical shear stress and erodibility coefficient relationship. But could not succeeded to develop the better relationship between these two parameters. Some other reasons have also been reported in the literature which involve predictive errors of up to an order of magnitude. Therefore,



**Fig. 8** Downstream view of groyne near Behlolpur (figure on left side, about 3 km downstream of Marala Barrage), downstream view of groyne (figure on right side, about 5 km downstream of Barrage)

**Fig. 9** Comparison and calibration of estimated and calculated bank erosion rate



many researchers have estimated the value of  $k_d$  from the calibration of the erosion results (Darby et al. 2010). Moreover, they suggested that the value of exponent “a” in Eq. (1) is not equal to unity because it is an empirically derived exponent.

Therefore, the erodibility coefficient relationship developed by Hanson and Simon (2001) was modified (i.e., by forcing best agreement between predicted using excess shear stress approach and calculated bank erosion using Landsat images). Similar approach is used to modify the relationship (Eq. 11) by many researchers (e.g., Rinaldi et al. 2008; Darby et al. 2007; Mosselman 1998). Equation 12 is the modified form of the Hanson and Simon relationship for estimation of the erodibility coefficient of river banks of the selected river reach:

$$K = 9 \times 10^{-7} \tau_c^{-0.5} \quad (12)$$

## Conclusions and recommendation

The calculated shear stress through numerical modeling was used in the excess shear stress approach to predict the river bank erosion along the right bank in the braided reach of River Chenab, Pakistan. The flows/flood events of 2010 were simulated using the two-dimensional numerical model. The predicted bank erosion by excess shear stress approach was compared with the one estimated from Landsat images. Modification in the erodibility coefficient in the Hanson and Simon (2001) model yielded better prediction of bank erosion. The scope of the study is limited by our focus on erosion by using the excess shear stress approach as the other bank erosion mechanisms have been ignored. Moreover, different sedimentary conditions of river banks have also been ignored. But it is explicit from the study that coupling of numerical model results with the excess shear stress approach is helpful in identification of the river bank locations more vulnerable to erosion which can further be useful for implementing protection structures along the river banks. The following points can be inferred from the coupled numerical model results with the excess shear stress approach:

1. Bank erosion estimation using the excess shear stress approach is greatly influenced by the erodibility coefficient. The best results for river bank erosion can be obtained by modifying the Hanson and Simon (2001) relationship for erodibility coefficient with critical shear stress. For this study, the bank erosion was estimated with good accuracy ( $R^2$  of 0.82) by using the modified relationship of the soil erodibility coefficient for the excess shear stress approach.
2. Protection works can be implemented at the locations which were identified more vulnerable to erosion on the basis of the results in the present study.
3. The minimum erosion and flow velocities downstream of the groyne suggest that the protection structures help to protect the river banks downstream of the bank by creating the recirculation zone which causes the sedimentation and eventually protects the river banks to erode.

For the present study, freely available Landsat images of 30-m resolution were used to calculate the bank erosion; therefore, it is recommended that the high-resolution satellite images should be used to analyze the difference of the bank erosion estimated with the freely available remote sensing images. River bank protection works may be implemented for similar reaches based on the computation of the model results. The erodibility coefficient for banks of different sediment sizes and different river patterns may be established to correctly estimate the erodibility coefficient with reasonable accuracy. Finally, it is recommended to analyze the impact of groyne height and length on the bank erosion for the river bank protection.

**Acknowledgements** This study was financially supported by the Higher Education Commission (HEC) of Pakistan within the framework of the Indigenous PhD fellowship Program. The financial support by HEC and institutional support by University of Engineering and Technology Lahore is gratefully acknowledged and appreciated. The authors also extend their thanks to the Punjab Irrigation Department (PID) for providing their survey and flow data. The paper greatly benefitted from the thorough reviews of anonymous referees.

## References

- Akhtar MP, Sharma N, Ojha CSP (2011) Braiding process and bank erosion in the Brahmaputra River. *Int J Sed Res* 26:431–444
- Arulanandan K, Gillogley K, R Tully (1980) Development of a quantitative method to predict critical shear stress and rate of erosion of natural undisturbed cohesive soils, Rep. GL-80-5, U.S. Army Corps of Eng., Waterways Exp. Station, Vicksburg, Miss
- Ashraf M, Bhatti MT, Shakir AS (2016) River bank erosion and channel evolution in sand-bed braided river reach of River Chenab: role of floods during different flow regimes. *Arabian J Geosci* 9(2):1–10
- Awan SA (2003) Pakistan: flood management-River Chenab from Marala to Khanki. Report on integrated flood management, Flood Forecasting Division, PMD
- Baki ABM, Gan TY (2012) Riverbank migration and island dynamics of the braided Jamuna River of the Ganges-Brahmaputra basin using multi-temporal Landsat images. *Quat Int* 263:148–161
- Clark LA, Wynn TM (2007) Methods of determining stream bank critical shear stress and soil erodibility: implications for erosion rate predictions. *Trans ASABE* 50(1):95–106
- Daly ER, Fox GA, Al-Madhhachi AT, Miller RB (2013) A scour depth approach for deriving erodibility parameters from Jet Erosion Tests. *Trans ASABE* 56(6):1343–1351
- Darby SE, Thorne CR (1996) Stability analysis for steep, eroding, cohesive river banks. *J Hydraul Eng* 122:443–454
- Darby SE, Rinaldi M, Dapporto S (2007) Coupled simulations of fluvial erosion and mass wasting for cohesive river banks. *J Geophys Res* 112:1–15
- Darby SE, Trieu HQ, Carling PA, Sarkkula J, Koponen J, Kumm M, Conlan I, Leyland J (2010) A physically based model to predict hydraulic erosion of fine-grained riverbanks: the role of form roughness in limiting erosion. *J Geophys Res* 115(F4). <https://doi.org/10.1029/2010JF001708>
- Ercan A, Younis BA (2009) Prediction of Bank Erosion in a reach of the Sacramento River and its mitigation with Groynes. *Water Resour Manag* 23:3121–3147
- Grissinger EH (1982) Bank erosion of cohesive materials. In: Hey RD, Thorne CR, Bathurst JC (eds) *Gravel-bed rivers*. Wiley and Sons, Chichester, pp 273–287
- Hanson GJ, Simon A (2001) Erodibility of cohesive stream beds in the loess area of the Midwestern USA. *Hydrol Process* 15:23–38
- Hooke JM (1979) An analysis of the processes of river bank erosion. *J Hydrol* 42:39–62
- Jia Y, Wang SSY (2001) CCHE2D: Two-Dimensional hydrodynamic and sediment transport model for unsteady Open channel flows over loose bed. Technical Report No. NCCHE-TR-2001-1
- Julian JP, Torres R (2006) Hydraulic erosion of cohesive river banks. *Geomorphology* 76:193–206
- Khan NI, Islam A (2003) Quantification of erosion patterns in the Brahmaputra-Jamuna River using geographical information system and remote sensing techniques. *Hydrol Process* 17:959–966
- Knighton AD (1974) Variation in width discharge relation and some implications of hydraulic geometry. *Geo Soc Am Bull* 85:1069–1076
- Lane EW (1955) Design of stable channels. *Trans Am Soc Civ Eng* 81(745):1–17
- Lawler DM (1992) Processes dominance in bank erosion systems, in lowland floodplain Rivers. In: Carling PA, Petts GE (eds) *Wiley*, New York, pp 117–143
- Luppi L, Rinaldi M, Teruggi LB, Darby SE, Nardi L (2009) Monitoring and numerical modelling of riverbank erosion processes: a case study along the Cecina River (central Italy). *Earth Surf Process Landf* 34(4):530–546
- Mosselman E (1998) Morphological modelling of rivers with erodible banks. *Hydrol Process* 12(8):1357–1370
- Mount NJ, Tate NJ, Sarker MH, Thorne CR (2013) Evolutionary, multi-scale analysis of river bank line retreat using continuous wavelet transforms: Jamuna River, Bangladesh. *Geomorphology* 183:82–92
- Osman AM, Thorne CR (1988) Riverbank stability analysis: I. Theory. *J Hydraul Eng* 114(2):134–150
- Partheniades E (1965) Erosion and deposition of cohesive soils. *J Hydraul Div* 91:105–139
- Rehman HU, Naeem UA, Nisar H, Ejaz N (2012) Development of empirical equations for the peak flood of the Chenab River using GIS. *Arab J Sci Eng* 37(4):945–954
- Rinaldi M, Mengoni B, Luppi L, Darby E, Mosselman E (2008) Numerical simulation of hydrodynamic and bank erosion in a river bend. *Water Resour Res* 44:1–17
- Simon A, Collison JC (2001) Pore-water pressure effects on the detachment of cohesive streambeds: seepage forces and matric suction. *Earth Surf Process Landf* 26(13):1421–1442
- Simon A, Pollen N, Mahacek V, Langendoen E (2009) Quantifying reduction of mass-failure frequency and sediment loading from stream banks using toe protection and other means: Lake Tahoe, United States
- Simon A, Pollen-Bankhead N, Thomas RE (2011) Development and application of a deterministic bank stability and toe erosion model for stream restoration. In: *Stream restoration in dynamic fluvial systems: scientific approaches, analyses, and tools*. American Geophysical Union, Washington DC, pp 453–474
- Sekely AC, Mulla DJ, Bauer DW (2002) Stream bank slumping and its contribution to the phosphorus and suspended sediment load of the Blue Earth River Minnesota. *J Soil Water Conserv* 57(5):243–250
- Shields IA (1936) Application of similarity principles and turbulence research to bed-load movement. In: Ott, WP, van Uchelen, JC (Eds.), (Translators), *Hydrodynamics Laboratory Publication*, vol. 167. California Institute of Technology, Pasadena
- Tariq MAUR, van de Giesen N (2012) Floods and flood management in Pakistan. *Phys Chem Earth* 47-48:11–20
- Thoma DP, Gupta SC, Bauer ME Kirchoff CE (2005) Airborne laser scanning for river bank erosion assessment. *Remote sensing of Env* 95:493–501
- Thoman RW, Niezgod SL (2008) Determining erodibility, critical shear stress, and allowable discharge estimates for cohesive channels: case study in the Powder River Basin of Wyoming. *J Hyd Eng* 134:1677–1678
- Takagi T, Oguchi T, Matsumoto J, Grossman MJ, Sarker MH, Matin MA (2007) Channel braiding and stability of the Brahmaputra River, Bangladesh, since 1967: GIS and remote sensing analyses. *Geomorphology* 85:294–305
- Thorne CR (1982) Processes and mechanisms of river bank erosion, in gravel-bed rivers, edited by R D Hey et al., pp. 227–271, John Wiley, Chichester, UK
- Van Rijn LC (1993) Principles of sediment transport in rivers estuaries and coastal seas. Aqua Publications, The Netherlands
- Wang S, Li L, Cheng W (2014) Variations of bank shift rates along the Yinchuan Plain reach of the Yellow River and their influencing factor. *J Geographical Sci* 24(4):703–716